J. Biochem. **134**, 239–244 (2003)
DOI: 10.1093/jb/mvg136

Crystal Structure of Chloroplastic Ascorbate Peroxidase from Tobacco Plants and Structural Insights into its Instability

Kei Wada[1], Toshiji Tada[*,1], Yoshihiro Nakamura[1], Takahiro Ishikawa[2], Yukinori Yabuta[3], Kazuya Yoshimura[3], Shigeru Shigeoka[3] and Keiichiro Nishimura[1]

[1]Research Institute for Advanced Science and Technology, Osaka Prefecture University, Gakuen-cho 1-2, Sakai, Osaka 599-8570; [2]Faculty of Life and Environmental Science, Shimane University, Matsue, Shimane 690-8504; and [3]Department of Food and Nutrition, Faculty of Agriculture, Kinki University, Nakamachi, Nara 631-8505

Received March 27, 2003; accepted May 29, 2003

Ascorbate peroxidase (APX) is a heme-containing protein that plays a central role in scavenging H_2O_2 in higher plants. The structure of stromal APX (sAPX) was determined at 1.6 Å to an *R*-factor of 19.1% and an *R*-free-factor of 22.3%. The electrostatic potential of the γ-channel that connects the molecular surface of sAPX to the γ-edge of heme was more positive than that of cytosolic APX (cAPX) from pea, so sAPX might bind more easily with ascorbate than cAPX. The overall structure of sAPX was similar to those of cAPX from pea and cytochrome *c* peroxidase (CCP) from yeast, with a substantial difference in a loop structure located in the vicinity of the heme. The side chain of Arg169 in sAPX corresponding to His169 in cAPX and His181 in CCP extended in the opposite direction from the heme, forming two hydrogen bonds with carbonyl groups in the loop structure. The rapid inactivation of sAPX might be due to the characteristic conformation of Arg169 owing to the loop structure of sAPX.

Key words: ascorbate peroxidase, chloroplastic isoenzyme, crystal structure, hydrogen peroxide, instability.

Abbreviations: APX, ascorbate peroxidase; AsA, ascorbate; sAPX, stromal ascorbate peroxidase; tAPX, thylakoid-bound ascorbate peroxidase; cAPX, cytosolic ascorbate peroxidase; mAPX, microbody-bound ascorbate peroxidase; CCP, cytochrome *c* peroxidase; MnP, manganese peroxidase; LiP, lignin peroxidase.

Ascorbate peroxidase (APX; EC 1.11.1.11) is a heme-containing protein that plays a central role in scavenging H_2O_2 to protect higher plants from oxidative stress (*1*, *2*). Under physiological conditions, APX is responsible for the rapid reduction of H_2O_2 to water at the expense of ascorbate (AsA) as a specific electron donor.

APX isoenzymes are distributed in at least four distinct cellular compartments, *i.e.* the stroma (sAPX) and thylakoid membrane (tAPX) of chloroplasts (*3*, *4*), microbodies (mAPX) including peroxisomes and glyoxysomes (*5*, *6*), and the cytosol (cAPX) (*7*, *8*). A fifth APX isoenzyme was found in mitochondria (*9*), although its molecular characteristics remain unknown. Interestingly, two chloroplastic APX isoenzymes are encoded by a single gene in various plant species such as spinach (*10–12*), pumpkin (*13*), *Mesembryanthemum crystallinum* (*14*), and tobacco (*14*), in which mRNAs are generated through the alternative splicing of two 3′-terminal exons. The sAPX and tAPX isoenzymes of tobacco plants, in particular, contain an open reading frame encoding mature proteins consisting of 295 and 344 amino acid residues with molecular masses of 33 kDa and 38 kDa, respectively. The 294 amino acid residues of sAPX excluding the C-terminal amino acid residue (Asp295) are identical with those of tAPX, which has extra 49 amino acid residues that comprise a putative transmembrane segment. In general, the kinetic parameters of sAPX are very close to those of tAPX with respect to the specificity for AsA and the K_m value for H_2O_2 (*3*, *11*, *15*, *16*).

One of the characteristics of chloroplastic APX isoenzymes is rapid inactivation in the absence of AsA (*15–19*). The isoenzymes from spinach lose their activities within several minutes when the AsA concentration is below 20 μM (*18*). In contrast, cAPX and mAPX are stable for at least several hours even under the conditions described above (*7*, *17*, *20*). Thus, AsA is suggested to have two functions, as a reducing agent for the catalytic reaction and as a stabilizer for the inactivation (*18*). The instability of the chloroplastic isoenzymes in AsA-depleted media was suggested to be due to the decomposition or elimination of the heme included in Compound I, which is a high oxidation-state intermediate, under conditions of excess H_2O_2 (*18*).

The peroxidase superfamily is classified into three major classes, I–III, based on sequence homology (*21*). Class I includes APXs of higher plants, catalase-peroxidases of microorganisms and cytochrome *c* peroxidase (CCP) of yeast. Class II includes manganese (MnP) and lignin peroxidases (LiP) of fungi, and class III includes classical secretory peroxidases represented by horseradish peroxidase. Among the class I peroxidases, yeast CCP has been the most extensively studied as to structure-function relations, because high-resolution structures have been determined for it (*22*). The crystal structure of a complex of CCP with cytochrome *c* might facilitate elucidation of the electron-transfer pathway, as mentioned by Pelletier and Kraut (*23*). However, CCP has limitations for use as a model for peroxidases, because it only

[*]To whom correspondence should be addressed. Tel: +81-72-254-9820, Fax: +81-72-252-6776, E-mail: tada@riast.osakafu-u.ac.jp

Table 1. **Summary of data collection and refinement statistics.**[a]

A. Data collection statistics[b]	
X-ray source	KEK-PF BL18B
Wavelength (Å)	1.0
Temperature (K)	100
Resolution (Å)	1.6 (1.69–1.60)
Space group	$P2_12_12_1$
Unit-cell parameters (Å)	a = 37.2, b = 76.8, c= 98.8
R_{merge} (%)[c]	6.6 (24.3)
$I/\sigma(I)$	8.0 (3.0)
Number of observed reflections	1,018,666
Number of unique reflections	37,796
Completeness (%)	98.9 (98.9)
Redundancy	6.5
Mosaicity (°)	0.3
B. Refinement statistics	
Resolution (Å)	8.0–1.6
R-factor (%)[c]	19.1
R-free-factor (%)[d]	22.3
C. Geometry statistics	
rmsd (bond distance) (Å)	0.006
rmsd (bond angle) (deg.)	1.3
Average B value (Å^2)	15.2
Ramachandran plot	
Most favored region (%)	92.1
Additionally allowed regions (%)	7.9

[a]The values for the highest resolution shell (1.69–1.60 Å) are given in parentheses. [b]From ref.25. [c]Rmerge = $\Sigma_{hkl}|I - \langle I\rangle|/\Sigma_{hkl}\langle I\rangle$; R-factor = $\Sigma||F_{obs}| - |F_{calc}||/\Sigma|F_{calc}|$. [d]R-free-factor calculated for 3,794 reflections (10%) was excluded from all refinements.

functions when cytochrome *c* is present as a specific electron donor. This is greatly different from almost all other well-studied peroxidases that oxidize small molecules.

Recently, the structure of pea cAPX was elucidated (*24*). Its structure led to a dichotomy of ideas, *i.e.* structural similarities with other peroxidases and dissimilarities with respect to the cation species involved (*24*). Thus, comparison of the structure of chloroplastic sAPX with those of CCP and cAPX should provide very important information regarding the characteristics. To obtain stereochemical information on the mechanism underlying the rapid inactivation of the APX isoenzyme, we carried out X-ray crystallographic analysis of the recombinant sAPX from tobacco plants, and compared its structure with those reported for CCP and cAPX.

MATERIALS AND METHODS

Crystallization, Data Collection, and Structure Refinement—Crystallization and data collection were described previously (*25*). In brief, sAPX was crystallized by the hanging-drop vapor-diffusion method using polyethylene glycol 4000 as a precipitant. The crystals belong to orthorhombic space group $P2_12_12_1$ with unit-cell parameters of a = 37.2 Å, b = 76.8 Å, c = 98.8 Å. A data set was successfully collected up to 1.6 Å resolution for a frozen crystal using synchrotron radiation of wavelength 1.0 Å at the BL18B station of KEK-PF. The intensity data were processed with program MOSFLM (*26*) and scaled using program SCALA (*27*). A summary of the data collection statistics is given in Table 1.

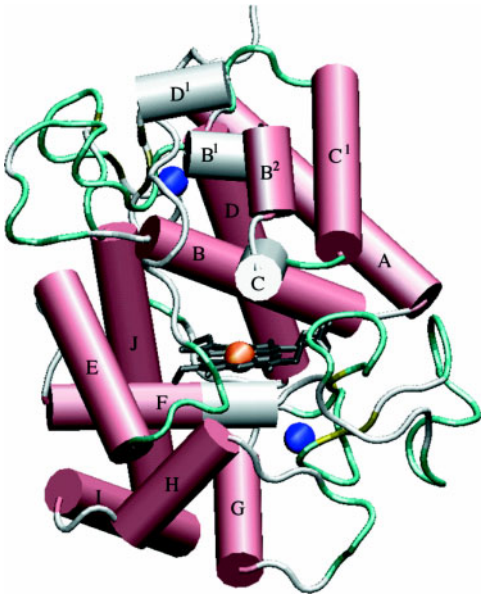

Fig. 1. **The structure of sAPX from tobacco plants.** The α- and 3_{10}-helices are shown as pink and white cylinders, respectively. The β-turns are shown in green and the hairpin in yellow. The iron atom and sodium ions are shown as orange and blue balls, respectively. The structure consists of domains I (helices A–D^1) and II (helices F–J). The structure was drawn using program VMD (*30*).

The initial phase was obtained using the molecular replacement procedure of CNS (*28*). The structure of pea cAPX (*24*), PDB entry 1APX, was used as a template. Subsequent refinement consisted of cycles of rigid-body positioning, positional minimization and B-factor optimization. Refinement was continued with simulated annealing refinement of CNS, followed by manual rebuilding of the structure in O (*29*). After the first round of refinement, amino acid substitutions were introduced into the model to convert it to the tobacco sAPX sequence, and the region exhibiting ambiguous density (last residues from the 17 C-terminus) was omitted from the model. The quality of the model was gradually improved by alternating rounds of refinement and model building until the R-free-factor value dropped to 25%. At this stage, ordered water molecules were added to the sAPX structure using the water-pick and -delete functions of CNS. Water molecules were kept if they were within hydrogen-bond capable distances, as determined by the contact protocol involving distance, geometry and neighbor constraints. The data collection and final refinement statistics are summarized in Table 1. The coordinates and structure factors have been deposited in the RCSB Protein Data Bank under accession code 1IYN.

RESULTS AND DISCUSSION

Description of the sAPX Structure—The final model was refined at 1.6 Å resolution. The asymmetric unit contains one protein molecule, two cations (modeled as sodium ions), and 296 water molecules. The whole structure of sAPX with protoporphyrin IX heme is shown in

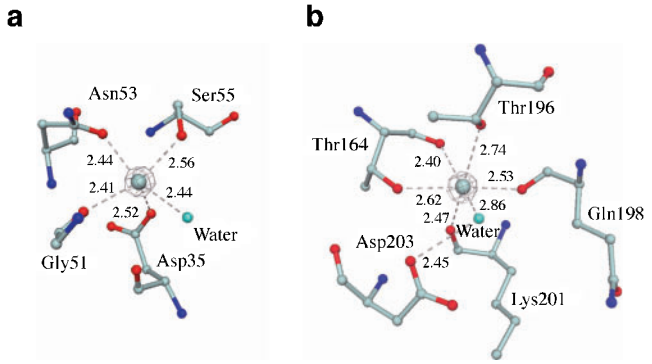

Fig. 2. **The environments around the binding sites with two cations; (a) the distal side and (b) the proximal side.** The positive electron difference densities were contoured at 7σ. The cation-ligand distances are given in Å. These structures were drawn using program DINO (*31*).

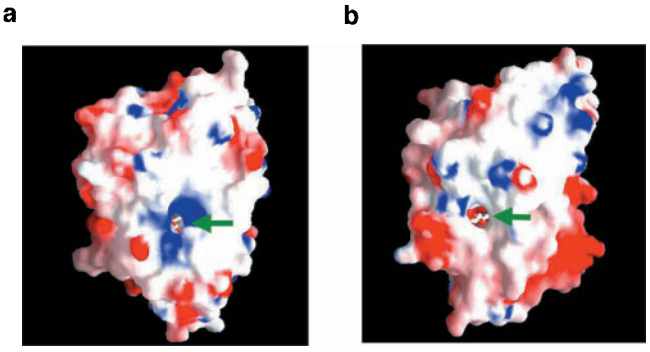

Fig. 3. **The electrostatic surface potentials for APX isoenzymes.** The channels are indicated by green arrows for the γ-channels of sAPX (a) and cAPX (b). Positive potentials are shown in blue and negative potentials in red. Molecular surfaces were generated and visualized with program GRASP (*39*).

Fig. 1. The 20 amino acid residues from the C-terminus were disordered and did not show sufficient electron density for assignments, because they might be located on the surface of the molecule. The topology of sAPX is very close to those of cAPX and CCP as a whole, and the helices of sAPX are designated according to the nomenclature of Finzel *et al*. (*22*). The structure consists of domains I (helices A–D[1]) and II (helices F–J), both of which are connected *via* the E-helix.

The F_o–F_c map of sAPX showed two peaks, one on the distal side and one on the proximal side. The peak on the distal side was surrounded by five oxygen atoms (Fig. 2a), while that on the proximal side was surrounded by six oxygen atoms (Fig. 2b). A carboxylate group (Asp35 for the distal side in Fig 2a; Asp203 for the proximal side in Fig. 2b) was found around each of the peaks. These findings clearly suggest that the peaks are derived from cations. The estimated cation-ligand distances are shown in Fig. 2. The average cation-ligand distance for the five bonds in Fig. 2a is 2.47 Å and that for the six bonds in Fig. 2b is 2.60 Å, both of which are within the reported range of Na^+-ligand distances, 2.4–2.6 Å (*32–34*). We further refined the structure by considering that these two sites are occupied by sodium ions, because the F_o–F_c maps did not show positive peaks when sodium ions were assigned to these two sites. The sodium ions should be incorporated from the reservoir solution used for crystallization. These temperature factors converged to appropriate values of 8.13 $Å^2$ and 8.96 $Å^2$. These two cation sites exhibit a good agreement, in fact, with those of two calcium ions in other peroxidases including *Arthromyces ramosus* peroxidase (*35*), LiP (*36*), and MnP (*37*).

Pea cAPX contains only one cation (K^+) on the proximal side (*24*), and CCP does not have any cation (*22*). One of the interesting aspects of pea cAPX is its sequence homology with CCP; cAPX contains the proximal side-Trp179 that corresponds to Trp191 in CCP. In CCP, Trp191 is suggested to be involved in a protein-based radical in Compound I, which is a high oxidation-state intermediate (*38*). In cAPX, however, the radical is judged to be in the porphyrin moiety (*24*). Patterson and Poulos (*24*) suggested that a potassium ion participates by increasing the electrostatic potential in the proximal heme pocket of cAPX, causing destabilization of the Trp radical. Thus, the radical of tobacco sAPX may be in the porphyrin moiety, because the location of the cation on the proximal side is close to that of the cAPX.

The Access Channel Connecting the Surface to the Heme Pocket—There are two access channels connecting the molecular surface with the distal heme pocket. They are connected with the δ- and γ-edges of the heme, so we refer to them as the δ- and γ-channels, respectively. The size of the γ-channel of sAPX (Fig. 3a) is close to that of cAPX (Fig. 3b), whereas the channels take different directions. The channel of cAPX is positioned approximately horizontal as to the heme plane, whereas the γ-channel of sAPX was positioned obliquely as to the heme plane (data not shown). In sAPX, the diameter of the channel is approximately 11.0 Å. The maximum size of an AsA molecule is approximately 7.1 Å, so AsA could enter the protein molecule through the γ-channel. The electrostatic potential of the channel in sAPX (Fig. 3a) is

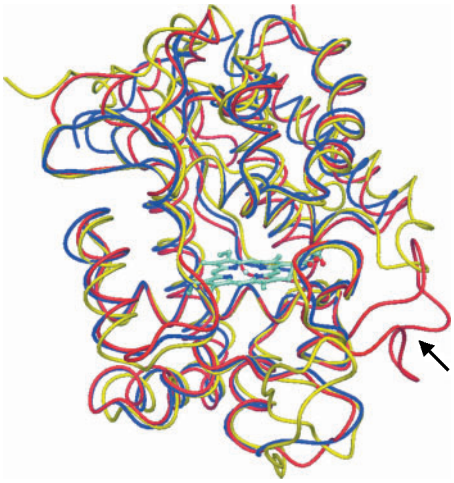

Fig. 4. **Superimposition of the C^α-traces of tobacco sAPX (red), pea cAPX (blue), and yeast CCP (yellow).** The arrow indicates the loop structure of sAPX. Superimposition was performed using program LSQKAB from the CCP4 program suite (*27*), and these structures were drawn using program DINO (*31*).

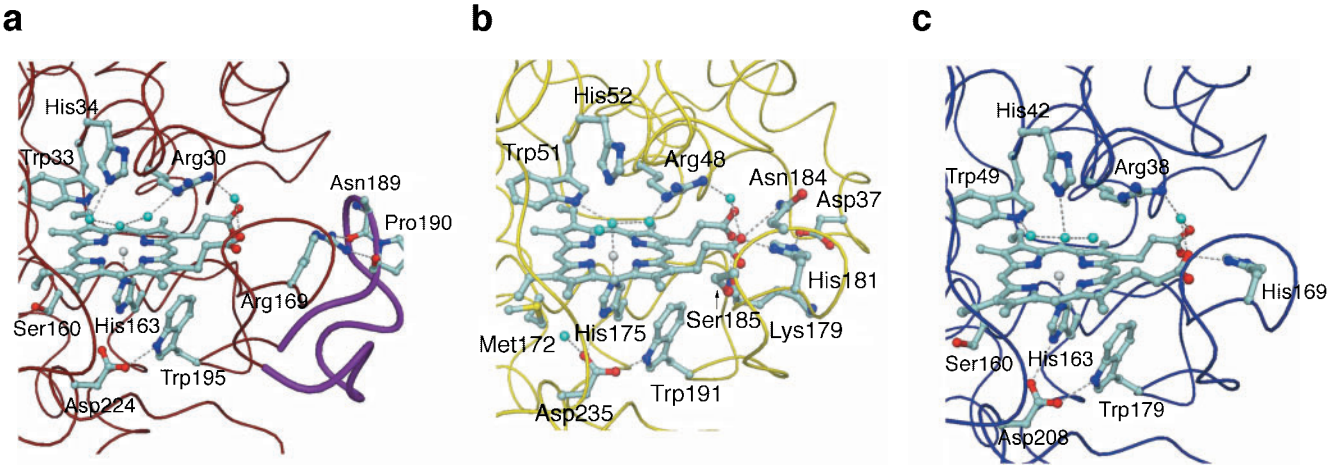

Fig. 5. **C^{α}-Traces for the active sites of tobacco sAPX (a), yeast CCP (b), and pea cAPX (c).** Only heme and key amino acid residues are shown as a ball-and-stick model. The Fe atom in the heme is shown in brown, nitrogen atoms in blue, oxygen atoms in red, the sulfur atom in yellow, and water oxygen atoms in cyan. Hydrogen bonds are indicated by broken lines. The loop structure in sAPX (a) is shown as a thick blue tube. These structures were drawn using program DINO (*31*).

more positively charged than that in cAPX (Fig. 3b). The negatively charged ascorbate anion might well electrostatically interact with the positively charged region, so that sAPX might bind more easily with AsA than cAPX. These findings agree well with the reported K_m values with AsA; 0.18 mM for sAPX (*16*) and 0.33 mM for cAPX (*7*).

Structural Insights into the Instability of sAPX—The structures of domains I and II of sAPX are very close to those of cAPX and CCP (Fig. 4). sAPX, but not cAPX or CCP, has a loop structure (residues 176–193) in the vicinity of the heme, as indicated by the arrow in Fig. 4. The loop structure consists of four β-turns (residues 180–183, 181–184, 183–186, and 187–190), and residues 167–194 form a hairpin structure.

In the active sites of these three peroxidases, the proximal His, and neighboring Asp and Trp have very close conformations. Furthermore, the distal His, and neighboring Arg and Trp functioning as a catalytic triad also have similar conformations (Fig. 5). The sAPX, however, has a characteristic conformation in the vicinity of the propionate side-chains of the heme (Fig. 5a).

In CCP, four amino acid residues (Lys179, Ser185, Asn184, and His181) participate in the formation of hydrogen bonds and a salt bridge with the propionate side-chains (Fig. 5b). Among these residues, His181 of domain II forms two hydrogen bonds with one of the propionate side-chains and with Asp37 of domain I to stabilize the enzyme through the interaction of domains, I and II. Indeed, the ability as to the structural change in Compound I is very small in CCP (*40*). The enzyme is very stable even when it is treated with excess H_2O_2 (*38*). In cAPX, which is more stable than sAPX in enzyme activity, His169 forms a salt bridge with one of the propionate side-chains of the heme, as in CCP. However, no hydrogen bond in this region was found to participate in the interaction between the domains (Fig. 5c). Therefore, it is conceivable that cAPX is somewhat unstable during the catalysis of oxidation reaction.

The most interesting and functionally important point about sAPX is that the side chain of Arg169 extends in the opposite direction from the propionate side-chains of the heme, and forms two hydrogen bonds with the carbonyl groups of Asn189 and Pro190 in the loop structure (Fig. 5a). However, no bonding was found to participate in the interaction between domains I and II in this region, as for cAPX. In addition, the propionate side-chains of the heme do not participate in the formation of a salt bridge and a hydrogen bond except for the bond with a water molecule (Fig 5a). Thus, the environments of the propionate side-chains of the heme in sAPX are greatly different from those of the other two peroxidases, cAPX and CCP. Miyake and Asada (*18*) found that the size of the Soret peak decreases with time when tAPX is treated with H_2O_2. They suggested that the inactivation of APX would result from degradation or elimination of the heme moiety.

Some mutants of a heme oxygenase from human, which degrades heme, exhibit peroxidase activity besides their own heme-degrading activity (*41*). In these mutants, some of the amino acid residues on the distal side changed to become homologous to those of peroxidases. Conversely, peroxidases may potentially have heme oxygenase activity. Applying these suppositions to sAPX, the inactivated enzyme may be a form in which the heme is movable and subsequently degraded by its own "heme oxygenase" activity. When sAPX is treated with AsA, the AsA molecule may bind with domains I and II and/or with the propionate side-chains to prevent the removal of the heme, resulting in the stabilization of the enzyme. These possibilities could be examined by analyses of the sAPX-AsA complex, as reported recently for soybean cAPX (*42*).

We wish to thank Professor N. Sakabe, and Drs. M. Suzuki, N. Igarashi and N. Matsugaki for their support in the data collection at KEK-PF, Japan. This work was performed with the approval of the Photon Factory Program Advisory Committee (Proposal No. 2002G140). This work was, in part, supported

by the Ministry of Agriculture, Forestry, and Fisheries of Japan (S.S.).

REFERENCES

1. Asada, K. (1992) Ascorbate peroxidase – a hydrogen peroxide-scavenging enzyme in plants. *Physiol. Plant.* **85**, 235–241
2. Shigeoka, S., Ishikawa, T., Tamoi, M., Miyagawa, Y., Takeda, T., Yabuta, Y., and Yoshimura, K. (2002) Regulation and function of ascorbate peroxidase isoenzymes. *J. Exp. Bot.* **53**, 1305–1319
3. Miyake, C., Cao, W.-H., and Asada, K. (1993) Purification and molecular properties of the thylakoid-bound ascorbate peroxidase in spinach chloroplasts. *Plant Cell Physiol.* **34**, 881–889
4. Asada, K. (1997) The role of ascorbate peroxidase and monodehydroascorbate reductase in H_2O_2 scavenging in plants in *Oxidative Stress and the Molecular Biology of Antioxidant Defenses* (Scandalios, J.G., ed.), pp. 715–735, Cold Spring Harbor Laboratory Press, New York
5. Yamaguchi, K., Mori, H., and Nishimura, M. (1995) A novel isoenzyme of ascorbate peroxidase localized on glyoxysomal and leaf peroxisomal membranes in pumpkin. *Plant Cell Physiol.* **36**, 1157–1162
6. Bunkelmann, J.R. and Trelease, R.N. (1996) Ascorbate peroxidase: A prominent membrane protein in oilseed glyoxysomes. *Plant Physiol.* **110**, 589–598
7. Mittler, R. and Zilinskas, B.A. (1991) Purification and characterization of pea cytosolic ascorbate peroxidase. *Plant Physiol.* **97**, 962–968
8. Ishikawa, T., Takeda, T., and Shigeoka, S. (1996) Purification and characterization of cytosolic ascorbate peroxidase from komatsuna (*Brassica rapa*). *Plant Sci.* **120**, 11–18
9. De Leonardis, S., Dipierro, N., and Dipierro, S. (2000) Purification and characterization of an ascorbate peroxidase from potato tuber mitochondria. *Plant Physiol. Biochem.* **38**, 773–779
10. Ishikawa, T., Yoshimura, K., Tamoi, M., Takeda, T., and Shigeoka, S. (1997) Alternative mRNA splicing of 3′-terminal exons generates ascorbate peroxidase isoenzymes in spinach (*Spinacia oleracea*) chloroplasts. *Biochem. J.* **328**, 795–800
11. Yoshimura, K., Yabuta, Y., Tamoi, M., Ishikawa, T., and Shigeoka, S. (1999) Alternatively spliced mRNA variants of chloroplast ascorbate peroxidase isoenzymes in spinach leaves. *Biochem. J.* **338**, 41–48
12. Yoshimura, K., Yabuta, Y., Ishikawa, T., and Shigeoka, S. (2002) Identification of a *cis*-element for tissue-specific alternative splicing of chloroplast ascorbate peroxidase pre-mRNA in higher plants. *J. Biol. Chem.* **277**, 40623–40632
13. Mano, S., Yamaguchi, K., Hayashi, M., and Nishimura, M. (1997) Stromal and thylakoid-bound ascorbate peroxidases are produced by alternative splicing in pumpkin. *FEBS Lett.* **413**, 21–26
14. Yoshimura, K., Yabuta, Y., Ishikawa, T., and Shigeoka, S. (2000) Expression of spinach ascorbate peroxidase isoenzymes in response to oxidative stresses. *Plant Physiol.* **123**, 223–233
15. Nakano, Y. and Asada, K. (1987) Purification of ascorbate peroxidase in spinach chloroplasts; its inactivation in ascorbate-depleted medium and reactivation by monodehydroascorbate radical. *Plant Cell Physiol.* **28**, 131–140
16. Madhusudhan, R., Ishikawa, T., Sawa, Y., Shigeoka, S., and Shibata, H. (2003) Characterization of an ascorbate peroxidase in plastids of tobacco BY-2 cells. *Plant Physiol.* (in press)
17. Chen, G.-X. and Asada, K. (1989) Ascorbate peroxidase in tea leaves: Occurrence of two isozymes and the differences in their enzymatic and molecular properties. *Plant Cell Physiol.* **30**, 987–998
18. Miyake, C. and Asada, K. (1996) Inactivation mechanism of ascorbate peroxidase at low concentrations of ascorbate; hydrogen peroxide decomposes compound I of ascorbate peroxidase. *Plant Cell Physiol.* **37**, 423–430
19. Yabuta, Y., Motoki, T., Yoshimura, K., Takeda, T., Ishikawa, T., and Shigeoka, S. (2002) Thylakoid-membrane bound ascorbate peroxidase is a limiting factor of antioxidative systems under photooxidative stress. *Plant J.* **32**, 15–25
20. Yoshimura, K., Ishikawa, T., Nakamura, Y., Tamoi, M., Takeda, T., Tada, T., Nishimura, K., and Shigeoka, S. (1998) Comparative study on recombinant chloroplastic and cytosolic ascorbate peroxidase isozymes of spinach. *Arch. Biochem. Biophys.* **353**, 55–63
21. Welinder, K.G. (1992) Superfamily of plant, fungal and bacterial peroxidases. *Curr. Opin. Struct. Biol.* **2**, 388–393
22. Finzel, B.C., Poulos, T.L., and Kraut, J. (1984) Crystal structure of yeast cytochrome *c* peroxidase refined at 1.7-Å resolution. *J. Biol. Chem.* **259**, 13027–13036
23. Pelletier, H. and Kraut, J. (1992) Crystal structure of a complex between electron transfer partners, cytochrome *c* peroxidase and cytochrome *c*. *Science* **258**, 1748–1755
24. Patterson, W.R. and Poulos T.L. (1995) Crystal structure of recombinant pea cytosolic ascorbate peroxidase. *Biochemistry* **34**, 4331–4341
25. Wada, K., Tada, T., Nakamura, Y., Yabuta, Y., Yoshimura, K., Takeda, T., Shigeoka, S., and Nishimura, K. (2002) Crystallization and preliminary X-ray diffraction analysis of chloroplastic ascorbate peroxidase of tobacco plants. *Acta Cryst.* **D58**, 559–561
26. Steller, I., Bolotovsky, R., and Rossmann, M.G. (1997) An algorithm for automatic indexing of oscillation images using Fourier analysis. *J. Appl. Crystallogr.* **30**, 1036–1040
27. Collaborative Computational Project, Number 4 (1994) *Acta Cryst.* **D50**, 760–763
28. Brünger, A.T., Adams, P.D., Clore, G.M., DeLano, W.L., Gros, P., Grosse-Kunstleve, W. *et al.* (1998) Crystallography & NMR system: A new software suite for macromolecular structure determination. *Acta Cryst.* **D54**, 905–921
29. Jones, T.A., Zou, J.-Y., Cowan, S.W., and Kjeldgaard, M. (1991) Improved methods for building protein models in electron density maps and the location of errors in these models. *Acta Cryst.* **A47**, 110–119
30. Humphrey, W., Dalke, A., and Schulten, K. (1996) VMD: Visual molecular dynamics. *J. Mol. Graphic.* **14**, 33–38
31. DINO: Visualizing structural biology (2001) http://www.dino3d.org
32. Thoden, J.B., Frey, P.A., and Holden, H.M. (1996) Molecular structure of the NADH/UDP-glucose abortive complex of UDP-galactose 4-epimerase from *Escherichia coli*: Implications for the catalytic mechanism. *Biochemistry* **35**, 5137–5144
33. Pelletier, H. and Sawaya, M.R. (1996) Characterization of the metal ion binding helix-hairpin-helix motifs in human DNA polymerase β by X-ray structural analysis. *Biochemistry* **35**, 12778–12787
34. Hall, D.R., Leonard, G.A., Reed, C.D., Watt, C.I., Berry, A., and Hunter, W.N. (1999) The crystal structure of *Escherichia coli* class II fructose-1, 6-bisphosphate aldolase in complex with phosphoglycolohydroxamate reveals details of mechanism and specificity. *J. Mol. Biol.* **287**, 383–394
35. Kunishima, N., Fukuyama, K., Matsubara, H., Hatanaka, H., Shibano, Y, and Amachi, T. (1994) Crystal structure of the fungal peroxidase from *Arthromyces ramosus* at 1.9 Å resolution: Structure comparisons with the lignin and cytochrome *c* peroxidases. *J. Mol. Biol.* **235**, 331–344
36. Doyle, W.A., Blodig, W., Veitch, N.C., Piontek, K., and Smith, A.T. (1998) Two substrate interaction sites in lignin peroxidase revealed by site-directed mutagenesis. *Biochemistry* **37**, 15097–15105
37. Sutherland, G.R.J., Zapanta, L.S., Tien, M., and Aust, S.D. (1997) Role of calcium in maintaining the heme environment of manganese peroxidase. *Biochemistry* **36**, 3654–3662
38. Erman, J.E. and Vitello, L.B. (1998) Cytochrome *c* peroxidase: A model heme protein. *J. Biochem. Mol. Biol.* **31**, 307–327
39. Nicholls, A., Bharadwaj, R., and Honig, B. (1993) Grasp: Graphical representation and analysis of surface properties. *Biophys. J.* **64**, A166
40. Fülöp, V., Phizackerley, R.P., Soltis, S.M., Clifton, I.J., Wakatsuki, S., Erman, J., Hajdu, J., and Edwards, S.L. (1994) Laue

diffraction study on the structure of cytochrome *c* peroxidase compound I. *Structure* **2**, 201–208
41. Liu, Y., Lightning, L.K., Huang, H.-W., Moénne-Loccoz, P., Schuller, D.J., Poulos, T.L., Loehr, T.M., and Ortiz de Montellano, P.R. (2000) Replacement of the distal glycine 139 transforms human heme oxygenase-1 into a peroxidase. *J. Biol. Chem.* **275**, 34501–34507
42. Sharp, K.H., Mewies, M., Moody, P.C.E., and Raven, E.L. (2003) Crystal structure of the ascorbate peroxidase-ascorbate complex. *Nat. Struct. Biol.* **10**, 303–307